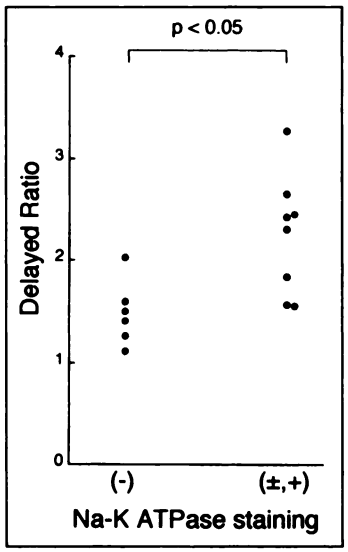

FIGURE 4. Correlation of Na-K ATPase and delayed ratios in adenocarcinomas of the lung.

thereby facilitating the prediction of prognosis, and provides insight into the relationship between ^{201}Tl uptake and malignancy.

REFERENCES

1. Strauss HW, Harrison K, Langan JK, Lebowitz E, Pitt B. Thallium-201 for myocardial imaging: relation of thallium-201 to regional myocardial perfusion. *Circulation* 1975;51:641–645.
2. Strauss HW, Boucher CA. Myocardial perfusion studies: lessons from a decade of clinical use. *Radiology* 1986;160:577–584.
3. Ochi H, Sawa H, Fukuda T, Inoue Y, Nakajima H. Thallium-201-chloride thyroid scintigraphy to evaluate benign and/or malignant nodules. *Cancer* 1982;50:236–240.
4. El-Desouki M. Thallium-201 thyroid imaging in differentiating benign from malignant thyroid nodules. *Clin Nucl Med* 1991;16:425–430.
5. El-Gazzar AH, Sahweil A, Abdel-Rahim SM. Experience with thallium-201 scintigraphy. *Clin Nucl Med* 1988;13:159–165.
6. Ramanna L, Waxman AM, Waxman S. Thallium-201 scintigraphy in bone and soft-tissue sarcoma: evaluation of tumor mass and viability [Abstract]. *J Nucl Med* 1988;29:854.
7. Tonami N, Shuke N, Yokoyama K, et al. Thallium-201 single photon emission computed tomography in the evaluation of suspected lung cancer. *J Nucl Med* 1989;30:997–1004.
8. Matsuno S, Tanabe M, Kawasaki Y, et al. Effectiveness of planar image and single photon emission tomography of thallium-201 compared with gallium-67 in patients with primary lung cancer. *Eur J Nucl Med* 1991;19:86–95.
9. Itoh K, Takekawa H, Tsukamoto E, et al. Single photon emission computed tomography using ^{201}Tl-chloride in pulmonary nodules: comparison with ^{67}Ga-citrate and ^{99m}Tc-labeled hexamethl-propleneamine-oxime. *Ann Nucl Med* 1992;6:253–260.
10. Suga K, Kume N, Orihashi N, et al. Difference in ^{201}Tl accumulation on single photon emission computed tomography in benign and malignant lesions. *Nucl Med Commun* 1993;14:1071–1078.
11. Sehweil AM, McKillop JH, Milroy R, Wilson R, Abdel-Dayem HM, Omar YT. Mechanism of ^{201}Tl uptake in tumors. *Eur J Nucl Med* 1989;15:376–379.
12. Kishida T. Mechanisms of thallium-201 accumulation to thryoid gland. *Kaku Igaku* 1987;24:991–1004.
13. Muranaka A. Accumulation of radioisotopes with tumor affinity II. Comparison of the tumor accumulation of ^{67}Ga-citrate and ^{201}Tl-chloride in vitro. *Acta Med Okayama* 1981;35:85–101.
14. World Health Organization. *Histological typing of lung tumors.* 2nd ed. Geneva: World Health Organization; 1981:25–26.
15. Saijo N, Niitani H, Tominaga K. Comparison of survival in nonresected well differentiated and poorly differentiated adenocarcinoma of the lung. *J Cancer Res Clin Oncol* 1980;97:71–79.
16. Takekawa H, Itoh K, Abe S, et al. Retention index of thallium-201 SPECT as an indicator of metastasis in adenocarcinoma of the lung. *Br J Cancer* 1994;70:315–318.
17. Takise A, Kodama T, Shimosato Y, Watanabe S, Suemasu K. Histopathologic prognostic factors in adenocarcinomas of the peripheral lung less than 2 cm in diameter. *Cancer* 1988;61:2083–2088.
18. Tonami N, Michigishi T, Bunko H. Clinical tumor scanning with ^{201}Tl-chloride. *Radioisotopes* 1976;25:829–831.
19. Oriuchi N, Tamura M, Shibazaki T, et al. Clinical evaluation of thallium-201 SPECT in supratentorial gliomas: relationship to histologic grade, prognosis and proliferative activities. *J Nucl Med* 1993;34:2085–2089.
20. Taguchi A. Clinical significance of thallium-201 single-photon emission computerized tomography (Tl-201 SPECT) in the evaluation of viability of gliomas. *Kurume Med J* 1992;39:267–278.
21. Caluser C, Macapinlac H, Healey J, et al. The relationship between thallium uptake, blood flow and blood-pool activity in bone and soft-tissue tumors. *Clin Nucl Med* 1992;17:565–572.
22. Ando A, Ando I, Katayama M. Biodistribution of ^{201}Tl in tumor bearing animals and inflammatory lesion induced animals. *Eur J Nucl Med* 1987;12:567–572.
23. Mountz JM, Raymond PA, Mckeeve PE, et al. Specific localization of thallium 201 in human high-grade astrocytoma by microautoradiography. *Cancer Res* 1989;49:4053–4056.
24. Elligsen JD, Thompson HEF, Kruuv J. Correlation of (Na-K)-ATPase activity with growth of normal and transformed cells. *Exp Cell Res* 1974;87:233–240.

Ultrasound-Guided Internal Radiotherapy Using Yttrium-90-Glass Microspheres for Liver Malignancies

Jia-He Tian, Bai-Xuan Xu, Jin-Ming Zhang, Bao-Wei Dong, Ping Liang and Xiang-Dong Wang

Departments of Nuclear Medicine and Ultrasound, The Great Wall Hospital, Beijing, China

Treatment of liver malignancies, in particular hepatocellular carcinoma, remains a serious problem because of the difficulty of delivering adequate therapeutic agents to the lesions while sparing the surrounding normal tissue. In an attempt to overcome this obstacle, intratumoral injection of ^{90}Y, a beta-emitter, was performed. **Methods:** Twenty-seven hepatocellular carcinoma's and six liver metastases were studied, most of which had failed other therapeutic modalities. Guided by ultrasound, ^{90}Y-glass microspheres (GMS) were carefully injected into predetermined tumor sites. The procedure was repeated at 3–4-wk intervals where indicated. Echographic, clinical and laboratory follow-up was conducted at regular intervals. **Results:** Twelve to 32 mo after treatment, 27 patients were still alive, with dramatic improvement of their clinical condition: 90.6% of the tumor foci became smaller, with echogenic or blood flow changes on liver sonograms. Serum titers of alpha-FP in 10 of 13 patients returned to normal levels. Repeat biopsy in nine patients showed complete tumor destruction in eight. Six patients died of either end-stage disease or wide dispersion of the tumor. **Conclusion:** The intratumoral administration of ^{90}Y-GMS under ultrasound guidance yielded a higher cure rate for liver malignancy with no severe side effects. The higher radiation dosage delivered by injected ^{90}Y to the periphery of the lesions (up to 28,215–75,720 cGy) was thought to account for the successful outcome. These results show that intratumoral radionuclide injection is feasible for treatment of malignant lesions inside the body.

Key Words: yttrium-90-glass microspheres; radionuclide therapy; liver malignancy; intratumoral delivery

J Nucl Med 1996; 37:958–963

Received Apr. 6, 1995; revision accepted Aug. 17, 1995.

For correspondence or reprints contact: Jia-He Tian, MD, Department of Nuclear Medicine, The Great Wall Hospital, Beijing, China 100853.

TABLE 1
Clinical Characteristics of 33 Study Patients

Patient no.	Sex	Age (yr)	Diag	No. of foci	Tumor size (cm)	^{90}Y-GMS		Other therapy	Pretherapy α-FP (ng/ml)	Post-therapy α-FP (ng/ml)	Comments
						No. of sessions	Total dose (mCi)				
1	M	62	HCC	1	2.6 × 2.4	2	20	A			
2	M	57	HCC	1	5.1 × 4.9	5	100	A	33	<10	ReB
3	M	58	HCC	2	3.2 × 2.2	3	30				ReB
4	F	65	Esop	2	3.2 × 4.2	4	75	C+A			
5	M	66	HCC	1	7.7 × 4.6	1	25	A+C			D (10 d)
6	M	58	HCC	1	6.1 × 4.6	5	100	A+C			
7	M	65	HCC	1	10.7 × 7.6	1	25	A+C			D (7 d)
8	M	52	HCC	1	8.6 × 8.8	6	120	A			
9	M	46	HCC	1	3.0 × 2.6	2	40				ReB
10	M	48	HCC	2	5.2 × 5.0	4	80	A+C			
11	M	67	Panc	1	3.3 × 2.6	2	30	A			
12	F	49	HCC	1	4.6 × 4.3	3	60		194	<25	
13	M	55	HCC	3	4.8 × 4.6	4	80	A+C	800	136	D (8 mo)
14	M	54	HCC	1	4.7 × 5.2	3	60	A+C			
15	M	50	HCC	—	—	2	35	C			D (2 mo)
16	M	65	HCC	1	2.8 × 2.2	2	25		195	69	ReB
17	F	44	Ovar	1	4.2 × 3.2	3	45				
18	M	49	HCC	1	1.8 × 2.0	1	10		713	<25	
19	M	65	HCC	1	3.2 × 2.6	2	60				
20	F	55	Rect	2	7.6 × 7.3 2.7 × 3.3	5	95				AMI (2 d)
21	M	61	HCC	2	4.6 × 4.8	4	60	C	136	25	
22	M	55	HCC	1	2.9 × 3.0	2	25		541	21	ReB
23	M	56	HCC	2	2.8 × 2.6 3.1 × 2.2	4	60	C			D (11 mo)
24	M	54	HCC	1	6.4 × 3.6	3	25		173.6	<25	ReB
25	M	70	HCC	1	4.5 × 3.9	3	45		191.7	<25	ReB
26	M	52	HCC	1	3.5 × 2.6	3	45		533	77	
27	M	43	HCC	1	4.3 × 4.0	3	45		81	<25	
28	F	58	HCC	1	2.5 × 1.9	1	20				
29	M	59	HCC	1	4.0 × 3.9	3	30		95	<25	ReB
30	M	58	HCC	1	6.1 × 5.4	5	75		80	<25	
31	M	39	HCC	1	8.2 × 7.9	6	120				ReB
32	M	44	Panc	1	6.0 × 4.7	4	70				
33	F	73	Colon	2	8.0 × 7.4 3.1 × 4.0	6	120				

Diag = diagnosis; HCC = hepatocellular carcinoma; A = 98% alcohol injection; ReB = repeat biopsy undertaken; Esop = metastases from esophagus; C = intraportal chemotherapy; D = died (time after treatment); Panc = metastases from pancreas; Ovar = metastases from ovaries; Rect = metastases from rectum; Colon = metastases from colon.

The incidence of liver malignancies, including hepatocellular carcinoma (HCC) and liver metastases, is very high in China. Patients with such tumors usually have a very poor prognosis because few treatment options are available. Only a limited number of patients are candidates for surgical resection, and although interventional therapy has been reported to be effective in some patients, the cure rate is still low and the clinical outcome unsatisfactory. The early dispersion and recurrence of tumor from malignant cells that remain after therapeutic attack are considered the major reasons for treatment failure. In an attempt to obtain better therapeutic results, internal radionuclide therapy using a high-energy beta-emitter, ^{90}Y, in the form of glass microspheres (^{90}Y-GMS), was introduced as a preferential agent for interventional therapy. Although most previous reports on the application of this agent used hepatic artery catheterization, in the present preliminary study, ^{90}Y-GMS was injected directly into liver tumors under ultrasound guidance. This intratumoral administration enabled higher irradiation doses to the tumor, with satisfactory results.

MATERIALS AND METHODS

Patients

Since May 1992, 33 patients with liver tumors have been referred to our laboratory for ultrasound-guided radionuclide therapy (26 men, 7 women; average age 56 yr, range 40–73 yr). The diagnosis had been confirmed by liver biopsy and included 27 HCCs and 2 metastases from the pancreas, 2 from the colorectum and 1 each from the esophagus and ovaries. By CT, MRI or ultrasound, single or multiple space-occupying lesions (SOLs) were identified in 24 and 8 patients, respectively, and the last patient was found to have a widespread lesion with no clearcut boundaries. The SOLs varied in size from 2.0 to 8.8 cm, but most were less than 5 cm in diameter (Table 1). In 84% of HCCs, underlying cirrhosis was also diagnosed. Patients with more than four SOLs in the liver were not considered suitable candidates for the current approach and thus were excluded from the study. Because of lesion location or size or unfavorable clinical conditions, most of these patients were not candidates for surgery. One patient had undergone hepatolobectomy at another hospital, but

widespread infiltrative tumor recurrence was found during a follow-up visit months later. Three patients showed no response but had side effects after intra-arterial embolizational chemotherapy. Written informed consent was obtained from each patient before entrance into the study; the study protocol was approved by this institution's ethics committee.

Treatment Protocol

The patient was supine on the table, under the ultrasound transducer, and was carefully positioned to ensure proper exposure of the lesion taking into account the operator's need for further manipulation. After local sterilization and anesthesia, percutaneous liver puncture was performed using a specially designed, modified 18-gauge biopsy needle. The tip of the needle was carefully directed to a predefined region of the tumor, 0.5–0.6 cm from its edge. Then, 74–92.5 MBq (2–2.5 mCi) ^{90}Y-GMS, suspended in 0.1–0.3 ml iodinated oil, was injected slowly into the tumor. For tumors larger than 3 cm, two to three injections were given, with the needle withdrawn in 1-cm steps. If needed, a second puncture was undertaken to achieve stereoscopic deposition of the radiosource throughout the tumor. For larger lesions, the procedure could be repeated at intervals of 3–4 wk to deliver doses to every portion of the tumor. For the safety of the patients, four to six doses per two to three punctures with 740–1,110 MBq (20–30 mCi) ^{90}Y-GMS in 1.0–1.5 ml oil were considered the limit for each treatment session. Tumors smaller than 5 cm usually required two to three sessions, whereas larger or multiple lesions required more. In the current group of patients, a maximum of six sessions was repeated in two patients with HCC and in one with liver metastases larger than 8 cm. After the procedure, the patients were asked to remain under supervision for 30 min before being dismissed, to ensure that no internal bleeding or adverse reaction occurred. Because the radiotracer remained in its injected position as a "point source," with no significant dispersion over the entire lifespan of the ^{90}Y, and was present in a spotty pattern, the radiation dose to the whole lesion was very difficult to calculate. Alternatively, the dose rate [R(x)] to the peripheral zone of the tumor from the point source that was considered the most clinically significant was calculated according to formula of Valley et al. (*1*):

$$R(x) = AnkE/4\pi\rho X_{90} \times F(\xi)/X^2,$$

where A = source activity (dps, or Bq); n is the number of beta-particles emitted (disintegrations); $k = 1.062 \times 10^{-8}$ rad · g^{-1}/MeV; E is the average energy of the beta-particles; ρ is the density of the tissue; X_{90} is the 90th percentile distance; $F(\xi)$ is the scaled absorption factor; and X is the distance between the source and the irradiated tissue.

The accumulated dose of the target tissue was determined by timing the dose rate according to the effective mean life of ^{90}Y-GMS in vivo. The latter was determined during scintigraphic surveillance of the patients after administration of ^{90}Y-GMS. The method has been validated by our own experience and by others (*7*) with animal experiments performed before the present clinical study.

To prevent extratumoral leakage of ^{90}Y-GMS, 11 patients underwent perilesional injection of 98% alcohol before the treatment session. In 10 patients, intraportal chemotherapy was undertaken as an adjutant means to prevent or treat portal metastases. The agents used were mitomycin-C, pharmorubicin 2 and 5-flurouracil. However, because these additional agents did not show any of the expected therapeutic gains but induced more side effects (e.g., pain, fever and leukopenia), both alcohol and chemical agents were abandoned midway through the study.

Monitoring and Follow-Up

Each patient underwent liver ultrasound at 1, 2 and 3 days; 1, 2 and 3 wk; and each month after therapy. Any changes in tumor radius, echogenicity and perfusion pattern on color Doppler mapping were checked and recorded. To quantify changes in size, a tumor shrinkage rate (TSR) was proposed and calculated as follows:

$$TSR = (L \times W - L' \times W')/(L \times W) \times 100\%,$$

where L(L′) and W(W′) are the maximum length and width of the lesion measured by the same experienced ultrasound physician (BWD) using the same machine before and after the treatment.

Immediately and at 1 and 2 days after each treatment session, a half-body scan from head to pelvis was performed using a large field of view gamma camera with a medium-energy, general-purpose collimator. On the basis of observations of the photon spectrum, the energy window was set at 80 keV with a 20% width for Bremsstrahlung scintigraphy of ^{90}Y-GMS distribution in the body. Regions of interest were set to obtain counts from the injected area and the adjacent liver, lungs and abdominal viscera.

The usual laboratory evaluations, including blood cell count and alpha-FP, GPT, AKP, gamma-GT, creatinine, blood urea nitrogen and serum protein levels, were performed periodically before and after treatment.

Nine patients underwent repeat biopsy of their SOLs at the third month after the last injection of ^{90}Y-GMS. These specimens were compared with those taken before treatment and with those from another 15 randomly selected patients who had undergone hepatic artery embolic chemotherapy in the radiology department. All pathological specimens were prepared in the same way and were reviewed and compared by the same two senior pathologists.

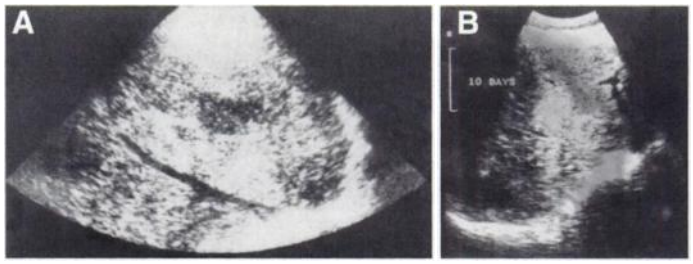

FIGURE 1. Ultrasound imaging of HCC before (A) and after (B) ^{90}Y-GMS injection. High echogenicity was obviously detected at the SOL, previously shown as a low-echogenic area.

RESULTS

Treatment

With real-time ultrasound monitoring, the tip of the inserted needle could be clearly delineated and guided to the proper location inside the SOL. Strong echogenicity was immediately depicted once the ^{90}Y-GMS injection started. The ^{90}Y-GMS could then be seen as echogenic spots seeded along the pathway of the needle as the latter was drawn into the SOL. Occasionally, the tracer could be seen "flowing" in some narrow, vessel-like gaps or even out of the SOL boundaries, which usually occurred after a fast, forceful injection. The distribution of the injected material remained stable throughout the entire procedure, but at follow-up, the strong echogenicity of ^{90}Y-GMS was gradually diminished and was finally replaced by the more uniform, high echogenicity of connective tissue (Fig. 1).

On the scintigram, the administered tracer appeared as a "hot spot," irregular in shape if multiple injections were given. In most cases, the whole liver was visible. The count ratio of hot spot to adjacent liver was roughly 8.6:1~32.2:1. In six patients, mild activity was also noted in the lungs, more obviously in the left lung (Fig. 2). The lesion/lung ratios were 4.8–11.3. Four patients had a small amount of activity in the intestines that disappeared within 1–2 days. No other organs were visualized.

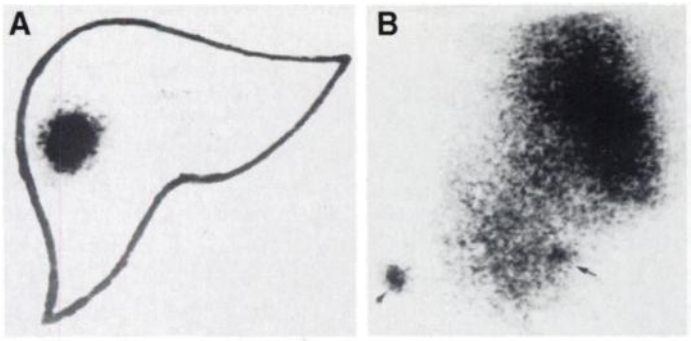

FIGURE 2. Bremsstrahlung imaging of liver and lungs from Patient 9 immediately after a normal injection (A) (injected activity appears as a "hot spot" within liver; no other organ showed any activity) and from Patient 6, who received an enforced injection (B). Injected radionuclide appears as a hot area in this large tumor, whereas activity in the left lung indicates leaching of the tracer. Because this patient was lying on the left side during injection, the tracer was driven to left lung by gravity. One ^{57}Co point source was placed on the sternum (arrow) and another on the lateral side of the thorax (arrowhead).

The hot spot remained stable in situ in all patients, and the measured half-life over the hot spot was 57.6 ± 1.02 hr. No activity higher than the background count was measured over the other organs.

The radiation dose at 0.5–0.8 cm from the source was calculated for an injected dose of 92.5 MBq (2.5 mCi), an effective half-life of 60 hr and related factors for ^{90}Y according to Berger (*2*) (Table 2).

Clinical Follow-Up

As of December 1994, 27 patients were still alive after a follow-up period of 12–32 mo (average 17.6 mo). All 27 patients showed clinical improvement: they had regained their body weight and physical strength, nutrition had improved, symptoms had subsided and they felt much better about themselves. Although intense but temporary liver pain and fever at 38.5–39.4°C for 2–3 days were reported after injection of alcohol/chemotherapy agents, no patient reported any unpleasant symptoms or signs related to ^{90}Y-GMS.

By the end of the follow-up period, only three patients with HCC showed signs of tumor progression in the lungs (three patients) or bone (one patient), despite a stabilized hepatic foci. These metastases were found at 11, 26 and 8 mo after the final injections.

Six patients died, two within 2 wk of initiation of treatment. Both of these patients had a late-stage, large hepatoma with severe cirrhosis, and one had previous hepatic artery embolizations, but ascites prevented further therapeutic attempts. Two patients died of metastases to the lungs, brain or pericardium, even though their primary liver foci were well controlled after treatment with ^{90}Y-GMS. One patient died of acute myocardial infarction the night after her second ^{90}Y-GMS treatment session. The last patient had undergone resection of his hepatoma about 9 mo previously and presented with diffused, ill-defined tumor recurrence on the sonogram, with carcinomatous thrombosis in the right portal vein. Despite a regional response to injected ^{90}Y-GMS, he died 2 mo after his second ^{90}Y-GMS treatment and several attempts of enhanced, intraportal chemotherapy. Follow-up in those patients still alive is ongoing.

TABLE 2
Absorbed Dose by Distance of Source

	Distance (cm)			
	0.5	0.6	0.7	0.8
F(ξ)	0.41	0.22	0.08	0.02
R(x) (cGy/sec)	0.35	0.13	0.03	0.007
Dose (cGy/G)	75,720	28,215	7,735	1,441

F(ξ) = scaled absorption factor; R(x) = dose rate.

Laboratory Findings

Among 13 patients with increased alpha-FP titer levels before treatment, 10 had normal test results (<25 ng/ml) at the latest follow-up visit. Three patients had decreased alpha-FP levels but abnormal test results, and one died 8 mo later. One patient showed an increase in alpha-FP levels during treatment after an initial decrease; a new focus was depicted weeks later and was treated with ^{90}Y-GMS, and alpha-FP levels declined again. No changes in other indicators of liver or renal function were detected. Two patients had a low white blood cell count after combined ^{90}Y-GMS and chemotherapy that improved within 1 mo.

Ultrasound Follow-Up

At final hepatic echocardiography in the surviving patients, 90.6% of the 32 foci treated had signs of tumor shrinkage. The TSR was 50% or more in 12 lesions, 25%–50% in another 12, less than 25% in 5, with no change in 3. During treatment, new foci were found in two livers, which were also treated by ^{90}Y-GMS and had the same response as the original foci.

Color Doppler flow mapping of the tumors after ^{90}Y-GMS also showed evidence of changes: 15 of 17 tumors showed a remarkable decrease in flow signal after treatment, 8 of which showed no flow at all, indicating either tumor necrosis or vascular occlusion.

Pathological Findings

Nine patients had a post-treatment biopsy at 3 mo after their last treatment session. At least three samples from various parts of the tumor bed were taken. In eight patients, no tumor cells could be found in any of the specimens, and the tumor tissue was completely replaced by fibrosis (Fig. 3 and 4). In contrast, pathological studies of samples from patients after hepatic artery interventions showed varying amounts of viable tumor cells in each case. The surviving tumor cells were more frequently found along the peripheral zone of the mass, regardless of the frequency of intervention. However, as a result of embolization, variable degrees of necrosis, fibrosis, vascular granulomatosis, capsulation and calcification could be seen.

DISCUSSION

Hepatocellular carcinoma, also known as hepatoma, trabecular carcinoma or carcinoma simplex, is one of the major malignancies encountered in China, Japan, The Philipines and Russia. According to World Health Organization statistics, of 6,350,000 cancer cases reported each year, 4% are HCCs, 42% of which occur in China (*3*). Usually, HCC is highly invasive, resulting in death in only months. Unlike other tumors, HCC shows very little, if any, response to ordinary chemotherapy or external beam radiotherapy. To physicians in China, therefore, treatment of HCC has remained a serious challenge (*4*).

Although surgical resection is still considered the best treatment, not every patient is a suitable candidate because of late diagnosis, multiple or widespread lesions, occult anatomic tumor location or adverse clinical conditions. In recent years, many alternatives have been suggested, such as interarterial infusion of chemotherapeutic agents and embolization of the artery supplying the tumor, with or without antitumor drugs. Although some encouraging results have been observed, there are still problems. One of the most clinically significant has

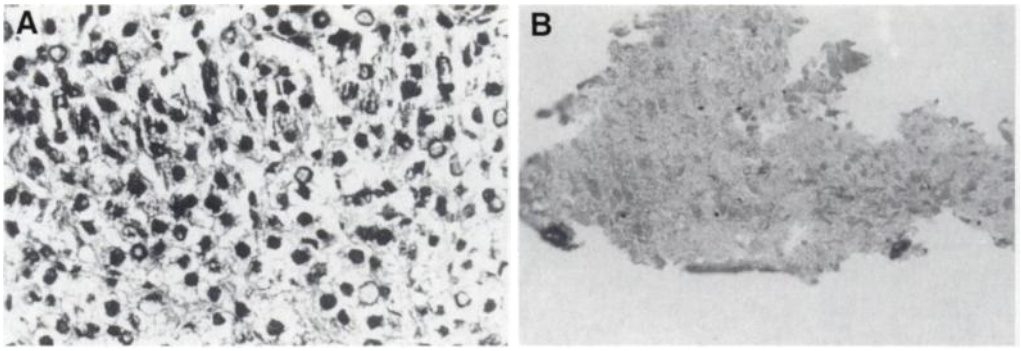

FIGURE 3. Biopsy specimen from a 46-yr-old patient with HCC (Patient) reveals a typical tumor before treatment (A); repeat biopsy (B) showed complete replacement of the tumor by fibrosis.

been the incomplete destruction of the HCC, even after the most enhanced therapy. Any viable tumor cells left, no matter the number or site of the remnants, could cause a recurrence of the tumor at a later time. Several factors could account for these cells surviving therapeutic attack. Some cells localized in the "shadow" of the antitumor agents because of low vascularity; some had a blood supply not only from the hepatic artery, but also from the portal system, enabling them to escape ischemia after embolization. There was even evidence that the portal system played an active role in at least some cases of HCC, which could be verified with color Doppler flow mapping. The portal blood supply was more evident at the boundary of the tumor and might even be enhanced after embolization (*5,6*). A better way to destroy every last tumor cell had to be found before a cure for HCC could be ensured.

Radionuclide internal radiotherapy is not a new idea. In the 1950s, ^{32}P and ^{198}Au were used to prevent and cure cancer in humans (*7*). In the past few years, ^{90}Y has been recommended as a preferential therapeutic agent. Obtained by neutron activation of stable ^{89}Y that has been integrated into glass microspheres, ^{90}Y-GMS has 64-hr half-life and 100% beta-emmission. The tracer is supplied in dry, solid form, 15–50 μm in diameter and is highly insoluble in either saline or body fluids. Therefore, ^{90}Y-GMS has a low risk of leaching out after interstitial injection, reducing the whole-body irradiation burden and with little effect on the reticuloendothelial system. Several clinical trials using ^{90}Y-GMS intra-arterially for HCC proved both the utility and safety of this agent (*5,7*). Yttrium-90, due to its short half-life and high energy ($\bar{E}_\beta$ = 0.93 MeV), delivers a higher dose rate than most other radionuclides used today. It has been shown that interventional therapy using radionuclides is somewhat superior than other agents because of the "neighboring" effect of the radiation (*5*). However, as mentioned by others, intra-arterial infusion of radionuclides does have some inherent drawbacks (*5,7*). First, the radionuclide reaches the tumor site by a nonspecific route, that is, it is passively carried by blood flow to a downstream field hosting both tumor and normal tissue. This means that normal tissue would be irradiated in the same way as the tumor, causing undesirable damage and limiting the total dose that could be delivered to the lesion itself. Second, because of the nonspecific distribution, large quantities of radionuclide must be used (e.g., 100–150 mCi or more). Third, this technique requires extremely selective catheterization and is therefore highly dependent on operator skill and equipment. Last, but not least, infusion of radionuclide cannot guarantee delivery of the proper dose to the peripheral zone of a lesion, where most of the surviving tumor cells localize.

As a result of these disappointing shortcomings of intra-arterial treatment, the direct injection of ^{90}Y-GMS into the tumor was utilized in the current study. Under real-time ultrasound guidance, ^{90}Y-GMS could be introduced to any tumor requiring irradiation. Less radioactivity, less normal tissue irradiation, less operator dependence, few side effects and better results have rendered the current modality a promising one.

In our previous animal experiments, we found that tumor tissue receiving an interstitial radiation dose higher than 176 Gy (17,668 rads) was completely destroyed. By the formula of Valley et al. (*1*), the dose rate to the periphery of the tumor, 0.5–0.6 cm from the source in our study, was about 0.27 cGy · g^{-1}/sec, making a total dose of up to 28,215–75,720 cGy, sufficient to kill all tumor cells. At distance of 0.8 cm, the dose decreased to 1,441 cGy, very tolerable by normal liver tissue. We were not concerned by doses to the tissue between 0.6 to 0.8 cm because they cause little or no damage to normal liver. In addition, it is not possible to definitely determine the location of the tumor edges. Once inside the body, ^{90}Y-GMS does not disintegrate or leach out, which was proved by the half-life derived from the gamma camera investigation. Thus, the tumor received almost all the radiation, whereas the adjacent normal tissue and other organs received very little, thus ensuring both safety and therapeutic efficacy, as demonstrated in our patients.

For any radiotherapy, the radiation dose delivered to the target is the major concern. In view of the different types of radiation (i.e., alpha-, beta-, gamma- or x-rays) and their biologic behavior, determination of the radiation dose for internal use of radionuclides is more complicated than for

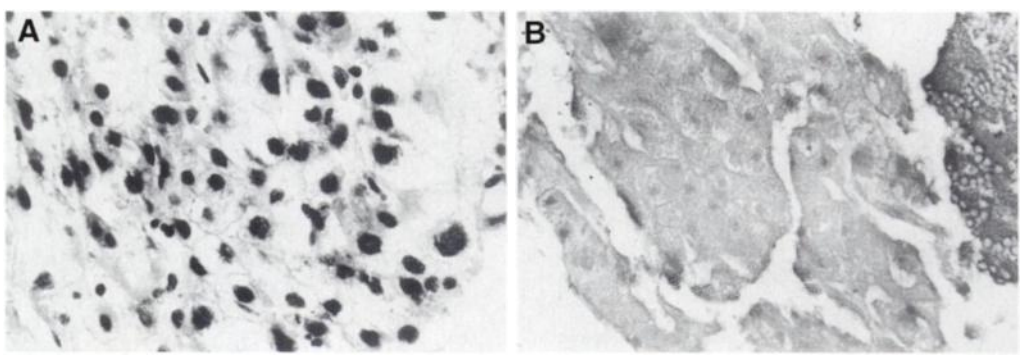

FIGURE 4. The same findings as in Figure 3 were seen in the biopsy specimen from a 65-yr-old patient with HCC (Patient 16) before (A) and after (B) treatment.

external radiotherapy. Unfortunately, in published reports to date, most of the formulas for internal radiation dose calculation have been based on the presumed uniform distribution of the radionuclide in the target. Such was definitely not the case in our interstitial use of ^{90}Y-GMS. In fact, several formulas suggested by others had indeed been adopted in our early trials, but the outcome of those calculations was confusing. With the same amount of tracer, the dose determined by different formulas varied from thousands to millions of rads. In view of the spotty distribution of ^{90}Y-GMS, it seemed more appropriate to calculate the dose according to the distance from the source. In fact, irradiation of the entire volume is not as critical as the dose to the peripheral region of the tumor because in our experience, most tumor remnants and extra blood supply exist in that region. With these findings in mind, we adopted the formula of Valley et al. (*1*), which is not concerned with the distribution pattern but calculates the dose rate for an area geometrically related to the source. Thus, we determined the doses for the peripheral zone of the tumor and ignored the central part. We hypothesized that once the cells at the periphery died, the central portion would die as a result of even stronger radiation. We believe that this policy resulted in the positive outcome of our study.

Although the dose that we used to treat our patients might seem to be much higher than any previously reported, we believed that the exclusive, stable and restrictive localization of ^{90}Y-GMS would result in regionalized irradiation. Additionally, the sharp contrast between internal and external radiotherapy was considered (*3*). Furthermore, no side effects were reported by our patients who received the current ^{90}Y-GMS dosage.

One of the benefits of ^{90}Y-GMS is its painlessness, in contrast to alcohol injection. There were no abnormal blood count or serum biochemical test results for hepatic and renal function. However, in a few patients, low-level lung radioactivity was detected by Bremsstrahlung scintigraphy. Whether this might cause pulmonary fibrosis over the long run, because these patients now have a better chance for survival, remains to be seen. However, it was previously believed that lungs receiving ^{90}Y-GMS of less than 10 mCi had no risk of severe side effects (*8*), and none of our six patients received more than 0.5–2.0 mCi in the lungs. In our experience, slow, gentle injection is the key to reducing adverse events in the lungs.

Careful review of the patients who died during the follow-up period clearly showed that at least two were at the end stage of their disease at the time of the first ^{90}Y-GMS injection. Both died within weeks, before irradiation could have an effect. This finding had been reported in some pioneering reports from the 1950s (*7*). It was suggested that to gain the expected result, it was necessary to start treatment as early as possible. Three of our patients died of widespread tumor metastases or invasion, indicating patients with multiple-organ involvement or with an infiltrative type of tumor might not be suitable candidates for treatment. The last patient died of acute myocardial infarction; however, it was not clear whether this event had any relation to the ^{90}Y-GMS injections because no autopsy studies were performed in this patient.

CONCLUSION

The principle of interstitial injection of a radionuclide could be applied to any organ or tissue, provided that safe and accurate delivery of the dose and intense monitoring could be ensured. Nevertheless, we are still at the early stages of the clinical experience, and a solid understanding of the factors behind the modality is lacking. Further study is warranted to determine the indications, contraindications, dose calibration, influencing factors, alternative solutions and rationale for interstitial radionuclide treatment.

ACKNOWLEDGMENTS

We thank Jin Xiao-hai, PhD, for supplying the ^{90}Y-GMS and Drs. Yu Guo, Yin Da-yi, Zhang Shu-wen and the staff of the nuclear medicine and ultrasound departments for their technical support.

REFERENCES

1. Valley JF, Kushelevsky AP, Lerch P. A method for the calculation of beta-ray dose. *Health Phys* 1974;26:295–300.
2. Berger MJ. MIRD pamphlet no. 7. Complete distribution of absorbed dose around point sources of electrons and beta particles in water and other media. *J Nucl Med* 1971;12(suppl 5):1–23.
3. Parkin DM, Stjernsward J, Muir CS. Estimates of the worldwide frequency of twelve major cancers. *Bull WHO* 1984;62:163.
4. Tang ZY. In: Tang ZY, Yang BH, eds. *Advances in Primary Liver Cancer Research*. Shanghai: Shanghai Medical University; 1990:1–8. In Chinese.
5. Yan ZP, Lin G, Dong YH, et al. An experimental study and preliminary clinical report on hepatoma treatment using ^{90}Y glass microsphere. *Chinese J Nucl Med* 1992;12: 220–222.
6. Honjo I, Suzuki T, Ozawa K, et al. Ligation of a branch of the portal vein for carcinoma of the liver. *Am J Surg* 1979;130:296–302.
7. Nakhgevany KB, Mobini J, Bassett JG, Miller E. Nonabsorbable radioactive material in the treatment of carcinomas by local injections. *Cancer* 1988;61:931–940.
8. Andrews JC, Walker SC, Ackermann RT, et al. Hepatic radioembolization with yttrium-90 containing glass microspheres: preliminary results and clinical follow-up. *J Nucl Med* 1994;35:1637–1644.

EDITORIAL

New Treatment Approaches to Liver Tumors

Traditional management of liver tumors typically has been surgical (*1*) when resectable, and chemotherapeutic when not resectable (*2–4*). Radiological procedures such as embolization, radio- and/or chemoembolization have been used in selected groups of patients in the U.S. and abroad (*5–8*).

Recently, a series of image-guided techniques that offer equivalent and, in certain tumors, better response than conventional therapies at a fraction of the cost have been developed and are under study. These techniques include percutaneous ethanol injection [now extensively in Europe and Asia in the treatment of hepatocellular cancer (*9,10*)], radiofrequency tumor ablation (*11*), image-guided cryosurgery (*12*) and interstitial laser photocoagulation (*13*).

In this issue of *JNM*, Tian et al. report on the novel use of image-guided, ^{90}Y-glass microsphere interstitial radiotherapy in the treatment of hepatic malignancies. This new technique extends the envelope of percutaneous brachytherapy as used in the prostate (*14*) and pelvis (*15*). Their results are quite encouraging.

To be accepted by the medical community, these new developments should undergo the same litmus test as the more traditional treatments [i.e., randomized studies need to be performed (*16*)]. There is little doubt that healthcare delivery systems will take note of these relatively simple, cost-effective, outpatient procedures that result in low morbidity and mortality. Therefore all concerned that

Received Feb. 21, 1996; accepted Mar. 1, 1996.

For correspondence or reprints contact: Jose F. Botet, MD, St. Agnes Hospital, Department of Radiology, 305 N. St., White Plains, NY 10605.